Introduction to Collisionless Single-Particle Motion in Plasmas

Jeremiah D. Williams[1] and A.M. Capece[2]
[1)] *Physics Department, Wittenberg University, Springfield, Ohio 45501, USA*
[2)] *Department of Physics, The College of New Jersey, Ewing, New Jersey 08628*

(*Electronic mail: capecea@tcnj.edu.)

(*Electronic mail: jwilliams@wittenberg.edu.)

(Dated: 9 June 2026)

Plasmas are the fourth and most common of the four naturally occurring states of matter observed in the universe, existing over a wide parameter space, with densities and temperatures spanning several orders of magnitude. As a result, a hierarchy of models is used to understand this state of matter, with the choice of model used determined by the plasma parameters and the level of detail required. The simplest of these models is single particle motion, which neglects interactions with other particles that make up the plasma, and considers only how individual particles respond to the presence of external electric and magnetic fields. Despite its simplicity, this model offers a rich insight into how charged particles respond to electromagnetic fields and underpins our understanding of more complex plasma behavior. In this tutorial, we explore the ways particles move under the influence of these fields using the Lorentz force as the governing equation of motion. Depending on the configuration of the fields, this model reveals a wide variety of behaviors, such as drifts and magnetic mirroring. We begin by analyzing motion in uniform fields, then extend the discussion to include nonuniform and time-varying fields. To build intuition, we present simulations that visualize the resulting trajectories. We also derive analytical expressions for key phenomena to complement and explain the simulated results. Finally, we highlight how these drift motions are relevant to plasmas of current interest, including those found in laboratory settings and in plasma confinement devices.

I. INTRODUCTION

Normal matter that is observed in the universe exists in one four fundamental states: solids, liquids, gases, and plasma.[1,2] The behavior of these states are defined by the underlying interactions that govern the motion of the components that make up a particular state of matter. For example, the behavior of a solid is defined by the interparticle interactions that result in the constituent atoms or molecules being rigidly fixed in space. As energy is added to the system, the kinetic (thermal) energy of the atoms or molecules increases until an energy barrier is passed. When this happens, the interparticle interactions are no longer large enough for the atoms or molecules to remain rigidly fixed in space and a phase transition is observed as the solid becomes a liquid. Similarly, if one considers a gas, such as air, the only interactions between the air molecules occur when they collide with each other. As a result, an air molecule will move in a straight line until it collides with another air molecule. If enough energy is added to a gas, another energy barrier is passed, at which point electrons are stripped from the individual atoms. This results in a conducting medium that, in addition to neutral atoms, contain electrons and (usually) positively-charged nuclei, *i.e.*, ions. While this state of matter is overall quasineutral, there can be spatially localized imbalances of charged particles. The electromagnetic interactions that arise from these local imbalances of charge lead to what is known as collective behavior, where the local behavior, or motion, of the particles in the system is determined not just by the local conditions mediated by collisions, but by conditions some distance away via electromagnetic interactions. For an introductory discussion of this topic, see the contribution by Schaffner[2] in this collection.

Most of the visible universe exists in the plasma state.[3] For example, stars, the interstellar medium and aurora are plasmas. Additionally, plasmas can be constructed for technological applications, and are used for electric propulsion, semiconductor manufacturing, lighting, medicine, and fusion reactors, among others.[4–6] For an introduction to fusion, see the contribution by Srinivasan[7] in this collection. Plasmas span a vast range of densities and temperatures, with comet tails having a low density and temperature, as compared with the solar corona, which is a hot, dense plasma. Since plasmas can exist over such a large parameter space, plasmas can exist in a regime where one can model their behavior by only considering the motion of individual particles, or plasmas can exist in a regime where collisions or interparticle interactions dominate and the plasma behaves more like a fluid.

To fully describe the behavior and evolution of a plasma, one must simultaneously and self-consistently compute three quantities: (1) the motion of the particles determined by the applied electric and magnetic fields, (2) the evolution of the current and charge densities based on the particle trajectories, and (3) how the electric and magnetic fields are modified based on the evolution of the current and charge densities. In practice, this is an impractical task, both analytically and computationally. As a result, plasma physicists have developed a hierarchy of models to understand these systems based on the parameters of the plasma (density, temperature, *etc.*) and the level of detail that is necessary. At one end of this hierarchy, one can employ the model of *single particle motion* where one ignores the interaction between the particles that make up the plasma and considers only how individual particles behave in external electric and magnetic fields. As the interactions between the plasma particles become important, including the particle interactions with the electric and magnetic fields that are generated by the moving plasma particles, tracking the motion of every individual particle becomes impossible. In this situation, one can replace the individual particles with a (smooth) distribution function, $f(\vec{r},\vec{v},t)$, and track the evolution of the distribution function over time instead of tracking the individual particles to understand the dynamics of the system. When the system is in thermal equilibrium (*i.e.* collisions dominate), the plasma particles will move together and the distribution function will not evolve in a significant way over short periods of time. In this case, one can simplify things by employing a fluid model where one takes moments of the distribution function to find the average behavior of particles filling a small volume of phase space, such as density, temperature, velocity, and pressure, which characterize the macroscopic properties of the system. This *fluid model* allows for a more complete and self-consistent description of a plasma. As the temperature of the plasmas increases, collisions can become rare and the plasma can remain out of thermal equilibrium for extended periods of time. In this situation, one can continue to track the evolution of the distribution function but cannot make the simplifying assumption of taking moments. This is the most complete (analytic) model of a plasma and is known as *kinetic theory*.

In the model of *single particle motion*, one assumes that the plasma particles do not interact with each other. In this case, the evolution of the particle's motion is governed by the externally applied electromagnetic fields experienced by the particle at a given instant in time. The simplicity of this approach might lead one to wonder if such a model would even be appropriate for a describing the behavior of a plasma, but it turns out that this approach can provide an understanding of many of the properties of a plasma and ultimately lays the foundation for understanding the emergence of collective behavior, where (Coulombic) particle interactions dominate. This model is particularly useful in systems where interactions between particles are minimal. One way to quantify this is by examining the average time between collisions (*i.e.* the inverse of the collision frequency), or equivalently, the average distance a particle travels before interacting with another particle, known as the mean free path, $\lambda_{\text{mfp, e}}$. When this time or distance is large compared to the characteristic timescales or length scales of the system, the single particle model becomes particularly useful. Such conditions are found in rarefied plasmas like the interstellar medium, in the radiation belts where particles are highly energetic, and in fusion plasmas. Table I summarizes typical plasma parameters (*e.g. electron density, n_e, and electron temperature T_e across different environments and calculates the relevant plasma quantities,* e.g. electron plasma frequency $\omega_{p,e} = \sqrt{\frac{q_e^2 n_e}{m_e \varepsilon_o}}$, electron-ion collision frequency $\nu_{ei} = n_e v_{\text{th},e} \sigma_{ei} \ln\Lambda$, the electron Debye length, $\lambda_{D,e}$, and the electron mean free path, $\lambda_{\text{mfp},e} = \frac{v_{th,e}}{\nu_{ei}}$, where Λ is the Coulomb logarithm, $v_{\text{th},e} = \sqrt{\frac{k_B T_e}{m_e}}$ is the electron thermal velocity and σ_{ei} is the electron-ion collision cross section, as described in Ref. [1].

The purpose of this tutorial is to explore a set of cases that demonstrate how the model of single particle motion can be used to understand key features of charged particle behavior in plasmas. It is intended for readers beginning to learn about this unique state of matter, who have a background in physics at the level of a second- or third-year undergraduate student and beyond. It is not intended to provide a comprehensive overview, and the reader is referred to many excellent textbooks that cover these motions in a more comprehensive fashion.[9–12] Simulations in VPython, where the equation of motion is solved using a fourth-order Runge-Kutta method to visualize particle trajectories, are presented and the related code is provided in the supplemental materials, allowing readers to apply these techniques to more complex scenarios and further develop their physical intuition. The structure of this manuscript is as follows: the governing ideas are summarized in Section II; examples involving uniform external fields are discussed in Section III; spatially non-uniform and time-varying fields are explored in Sections IV and V, respectively. A summary is then provided in Section VI.

II. FUNDAMENTALS OF PARTICLE MOTION

When the charged particles in a plasma do not significantly interact with each other, the motion of each particle can be treated independently. In these situations, the charge and mass of the plasma particles (ions, electrons) result in electromagnetic interactions, described by the Lorentz Force Law, being the dominant forces and the motion of the particles can be described by applying Newton's 2nd Law, Eq. 1.

$$\vec{F} = m\vec{a} = q\left(\vec{E} + \vec{v}\times\vec{B}\right), \tag{1}$$

where m is the particle mass, q is the particle charge, $\vec{E}$ is the electric field, $\vec{v}$ is the particle velocity, and $\vec{B}$ is the magnetic field. The Lorentz force equation, given in Eq. 1, captures the fundamental physics needed to describe particle motion in externally applied electric and magnetic fields. It is often useful to decompose the velocity of the particle into components parallel, $v_\parallel$, and perpendicular, $v_\perp$, to the magnetic field:

$$\vec{v}_\parallel = \frac{\vec{v}\cdot\vec{B}}{B}\hat{B}, \tag{2}$$

$$\vec{v} = \vec{v}_\parallel + \vec{v}_\perp. \tag{3}$$

where $\hat{B}$ is a unit vector that points in the direction of the magnetic field.

III. UNIFORM ELECTRIC AND MAGNETIC FIELDS

A. Case 1: Uniform Magnetic Field

As a starting point, let's consider the case of an ion or electron with charge q and mass m in a region of uniform magnetic field, $\vec{B} = B_o\hat{z}$ and no electric field, $\vec{E} = 0$. In this situation, we see from Eq. 1 that the force is perpendicular to both the direction of motion, $\hat{v}$, and the applied magnetic field, $\hat{B}$. Because of this, we would expect that the plasma particle will exhibit

TABLE I. Typical plasma parameters for a range of plasma systems calculated using the PlasmaPy library.[8] The primary gas species for each plasma is indicated in parentheses. The inverse of the collisions frequency, ν_{ei}, or the distance traveled between collisions, $\lambda_{\mathrm{mfp,e}}$, can be useful in determining the appropriate model to use. Based on these values, one would expect that the model of single particle motion would be most useful in describing the first four examples.

Plasma	n_e (m^{-3})	T_e (eV)	$\omega_{p,e}$ $\left(\frac{\mathrm{rad}}{\mathrm{s}}\right)$	ν_{ei} (Hz)	$\lambda_{\mathrm{D,\,e}}$ (m)	$\lambda_{\mathrm{mfp,\,e}}$ (m)
Interplanetary Medium (H)	10^6	1	10^5	10^{-5}	10	10^9
Earth's Ionosphere (O)	10^{11}	0.1	10^7	10^2	10^{-2}	10^3
Earth's Outer Magnetosphere (H)	10^6	3	10^3	10^{-5}	10^1	10^{10}
Fusion Experiment (H)	10^{19}	10^4	10^9	10^2	10^{-5}	10^3
gas disharge (Ar)	10^{15}	2	10^9	10^4	10^{-4}	10^3
Solar corona (H)	10^{13}	10^2	10^8	10^0	10^{-2}	10^6

uniform circular motion about the magnetic field. To be more quantitative, we can write Eq. 1 in Cartesian coordinates as

$$\frac{dv_x}{dt} = \dot{v}_x = \frac{qB_0}{m} v_y \tag{4a}$$

$$\frac{dv_y}{dt} = \dot{v}_y = -\frac{qB_0}{m} v_x \tag{4b}$$

$$\frac{dv_z}{dt} = \dot{v}_z = 0, \tag{4c}$$

where we have introduced a short-hand notation for the time derivative, in which each dot over a quantity represents a time derivative of that quantity, *e.g.* $\dot{v}_z = \frac{dv_z}{dt}$. From Eq. 4c, we see that the motion of the plasma particle does not change in the direction parallel to the magnetic field, which is $\hat{z}$ for this example. As such, a particle that has a component of velocity in the direction of the magnetic field will drift with a constant velocity, $v_\parallel$. From Eqs. 4a and 4b, we see that the motion in the x and y directions are coupled. To decouple these equations, we first take the time derivative of Eq. 4a to obtain an expression for $\ddot{v}_x$, which we then combine with Eq. 4b to arrive at Eq. 5a. Applying the same process to Eq. 4b leads to Eq. 5b:

$$\ddot{v}_x = \frac{qB_o}{m}\dot{v}_y = -\left(\frac{qB_o}{m}\right)^2 v_x = -\omega_c^2 v_x, \tag{5a}$$

$$\ddot{v}_y = -\frac{qB_0}{m}\dot{v}_x = -\left(\frac{qB_0}{m}\right)^2 v_y = -\omega_c^2 v_y, \tag{5b}$$

Here, we see that the plasma particle undergoes harmonic motion about the magnetic field line at a gyrofrequency given by $\omega_c = \frac{|q|B_0}{m}$ with a direction that depends on the sign of the particle's charge. This frequency, ω_c, is known as the cyclotron frequency and quantifies the rate at which a charged particle orbits the magnetic field. The gyroradius of the orbit, known as the Larmor radius r_L, can be found by noting that the magnetic force is centripetal, so $\frac{mv_\perp^2}{r} = q \mid \vec{v} \times \vec{B} \mid = qv_\perp B_0$, or

$$r_L = \frac{mv_\perp}{qB_0} = \frac{v_\perp}{\omega_c}. \tag{6}$$

Figure 1 shows a simulation for a particle with an initial velocity in the x and z directions. Notice that the particle exhibits circular motion in the x-y plane and drifts in the $+z$ direction, along the magnetic field. The gyration represents a microcurrent which creates a magnetic field that is opposite to the applied background field, making plasmas a diamagnetic material.

The exact motion of the particle can be found by integrating Eqs. 5a and 5b to yield:

$$x(t) - x_{gc} = r_L \sin(\omega_c t + \phi_0) \tag{7a}$$

$$y(t) - y_{gc} = \pm r_L \cos(\omega_c t + \phi_0), \tag{7b}$$

where x_{gc} and y_{gc} describe the x and y coordinates of the center of the orbit, and ϕ_0 is an arbitrary phase to match the initial conditions. Eq. 7 describes a particle moving in a circular orbit around the magnetic field line centered at the guiding center with a gyroradius, r_L, and gyrofrequency, ω_c. A schematic of this gyromotion in the x-y plane is shown in Fig. 2.

The motion of charged particles in a magnetic field can be thought to consist of the linear motion of the guiding center superimposed on circular motion *about* the guiding center. In Fig. 1, $\phi_0 = \pi/2$, and the guiding center of the particle is fixed in x and y, but increases linearly with time in z: $(x_{gc}, y_{gc}, z_{gc}) = (x_0, 0, v_{z_0} t)$.

B. Case 2: Uniform Electric and Magnetic Fields

Now, let's consider the case of a charged particle in a region of uniform electric, $\vec{E} = E_x\,\hat{x} + E_y\,\hat{y} + E_z\,\hat{z}$, and magnetic, $\vec{B} = B_0\,\hat{z}$, field. In this case, it is easiest to qualitatively see what happens by decomposing the electric field into its components parallel, $\vec{E}_\parallel = E_z\,\hat{z}$, and perpendicular,

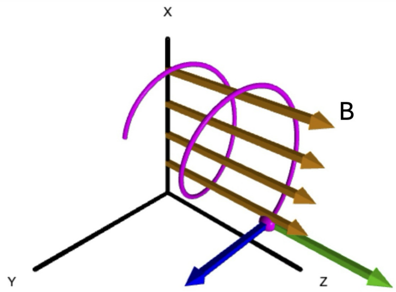

FIG. 1. Plot of the trajectory of a proton with an initial position and velocity of $\vec{x}_0 = 0.08\,\hat{x} + 0.05\,\hat{y} + 0\,\hat{z}$ m and $\vec{v}_0 = 5\times10^5\,\hat{x} + 0\,\hat{y} + 1\times10^5\,\hat{z}$ m/s, respectively, traveling in region where the magnetic field is $\vec{B} = 0.1\,\hat{z}$ T. The particle traces out a helical trajectory as it moves along the magnetic field. The green and blue arrows indicate $v_\parallel$ and $v_\perp$, respectively.

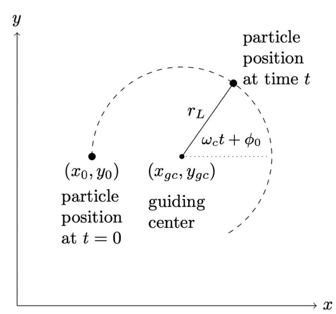

FIG. 2. A charged particle moving in a magnetic field undergoes circular motion about its guiding center.

$\vec{E}_\perp = E_x\hat{x} + E_y\hat{y}$, to the magnetic field. In this situation, we expect that the particle will exhibit gyromotion in the x-y plane due to the magnetic force and will move with a constant acceleration in the z-direction due to the electric force from $\vec{E}_\parallel$. To understand the effect that the perpendicular component of the electric field has, let's assume that the plasma particle has a positive charge. In this case, the particle will experience a positive acceleration (*i.e.* speed up) when it is moving in the positive x and y directions and experience a negative acceleration (*i.e.* slow down) when it is moving in the negative x and y directions due to the electric force from $\vec{E}_\perp$. This will result in a guiding center drift in the direction perpendicular to both $\vec{E}$ and $\vec{B}$. To be more quantitative about this, let's apply the Lorentz force equation in its component form:

$$\dot{v}_x = \frac{qE_x}{m} + \frac{qB_0}{m}v_y = \frac{qE_x}{m} + \omega_c v_y \tag{8a}$$

$$\dot{v}_y = \frac{qE_y}{m} - \frac{qB_0}{m}v_x = \frac{qE_y}{m} - \omega_c v_x \tag{8b}$$

$$\dot{v}_z = \frac{qE_z}{m}. \tag{8c}$$

As expected, we see that the particle experiences a constant acceleration, $\frac{qE_z}{m}$, in the $\hat{z}$ direction. The motion in the x- and y-directions can be decoupled by taking the time derivative of Eqs. 8a and 8b, which leads to

$$\ddot{v}_x = \omega_c \dot{v}_y = -\omega_c^2\left(v_x - \frac{E_y}{B_0}\right) \tag{9a}$$

$$\ddot{v}_y = -\omega_c \dot{v}_x = -\omega_c^2\left(v_y + \frac{E_x}{B_0}\right). \tag{9b}$$

Integrating Eq. 9, we find the motion of the particle to be

$$x(t) = r_L \sin(\omega_c t + \phi_0) + \frac{E_y}{B_0}t \tag{10a}$$

$$y(t) = r_L \cos(\omega_c t + \phi_0) - \frac{E_x}{B_0}t, \tag{10b}$$

where ϕ_0 is again an arbitrary phase to match the initial conditions. The resulting motion is similar to the case of uniform $\vec{B}$ with $\vec{E} = 0$; however, the guiding center now experiences a motion given by $\vec{x}_{gc} = \left(\frac{E_y}{B_0}t\,\hat{x} - \frac{E_x}{B_0}t\,\hat{y}\right)$. This corresponds to a constant drift velocity, known as the $\vec{E}\times\vec{B}$ drift velocity, that is independent of the charge and can be written in vector form as:

$$\vec{v}_{E\times B} = \frac{\vec{E}\times\vec{B}}{B^2}. \tag{11}$$

This result, Eq. 11, can be generalized by replacing the electric field in Eq. 8 with a field that represents an arbitrary, constant force, $\frac{\vec{F}}{q}$, and observe that any external force will result in a drift given by

$$\vec{v}_D = \frac{\vec{F}\times\vec{B}}{qB^2}. \tag{12}$$

To make sense of this motion, described by Eq. 10, let's simplify things by considering the case when $E_x = 0$. In this case, the motion can be described using Eq. 13.

$$x(t) = r_L \sin(\omega_c t + \phi_0) + v_d t \tag{13a}$$

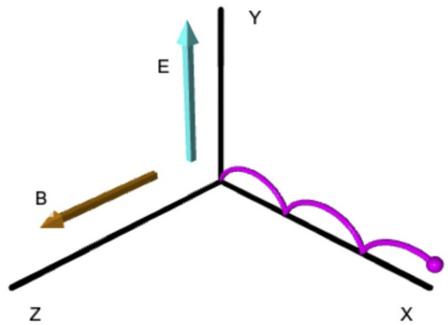

FIG. 3. Plot of the trajectory of a proton starting from rest at the origin in q region where the electric field is $\vec{E} = E_0\,\hat{y}$ and magnetic field is $\vec{B} = B_0\,\hat{z}$. The particle traces out a cycloidal trajectory and drifts in the $\vec{E}\times\vec{B}$ direction.

$$y(t) = r_L \cos(\omega_c t + \phi_0), \tag{13b}$$

where $v_d = \frac{E_y}{B_0}$ represents a drift speed. Here, we see that the particle traces out a cycloid whose shape is determined by the ratio of the drift speed to the gyroradius speed, $v_\perp$. If $v_d < v_\perp$, the path of the particle is described by a *curtate* cycloid (a pointed loop/cusp). On the other hand, if $v_d > v_\perp$, the path of the particle is described by a *prolate* cycloid (a looping trail). This motion can also be visualized with a simulation, Fig. 3. Here, we examine the motion a proton in electric and magnetic fields with $\vec{B} = B_0\,\hat{z}$ and $\vec{E} = E_0\,\hat{y}$. Notice that the particle drifts in the $+x$-direction, consistent with Eq. 11, and we observe that $v_d < v_\perp$.

This leaves us with a *key takeaway*: the effect of uniform external fields on a charged particle is a net drift motion of the guiding center superimposed on the gyromotion about the guiding center due to the external magnetic field. This can be expressed as

$$\vec{x} = \vec{x}_{gc} + \vec{r}_L \tag{14a}$$

$$\vec{v} = \vec{v}_{gc} + \vec{v}_L, \tag{14b}$$

where $\vec{x}_{gc}$ and $\vec{v}_{gc}$ represent the position and velocity of the guiding center relative to the coordinate origin, and $\vec{x}_L$ and $\vec{v}_L$ represent the position and velocity of the particle relative to the guiding center.

Application: The $\vec{E}\times\vec{B}$ drift plays a critical role in the subfield of nonneutral plasmas,[13] which consist of only one type of charged particles. These plasmas can be created in a number of geometries, but one of the simplest is known as a Penning trap.[14] This device consists of three coaxial, conducting cylinders that are axially aligned with the inner and outer cylinders biased to a positive voltage relative to the middle cylinder. This creates a radial electric field that increases outward from the center of the device. In addition, a strong external magnetic field, $|B| \geq 1$ T, that is aligned along the axis of the device is applied. This configuration results in an $\vec{E}\times\vec{B}$ drift velocity, Eq. 11, that increases as you move radially away from the center of the device, causing ions or electrons to rotate as a rigid body and allowing for extended confinement times.

IV. NONUNIFORM MAGNETIC FIELDS

In Section III, we saw that the motion of a particle in uniform electric and magnetic fields results in a net drift motion of the guiding center superimposed on the gyromotion *about* the guiding center due to the external magnetic field. We also saw that any constant force with a component perpendicular to the magnetic field will induce a drift according to Eq. 12.

In reality, however, most magnetic fields are not uniform, and the strength and direction of the field varies from location to location, and this spatial variation in the magnetic field will result in forces that influence charged particle motion. In these cases, particles will experience forces as a result of gradients in the field strength and curvature of the field lines. Particles may experience "mirroring" as they move from regions of lower to higher magnetic field strength, causing them to reflect back along their original path. These phenomena, which will be discussed in more depth in this section, are important for fusion devices, magnetic mirror traps, and for particles in Earth's magnetosphere, where particle motion strongly depends on magnetic field structure. Provided that electric and magnetic fields remain approximately uniform and steady over a cyclotron orbit, we can extend the model from Section III to analyze the motion in more complex fields by considering the motion of the particle to consist of two parts: the slow motion of the local guiding center and the fast oscillating cyclotron motion about the guiding center as described in Eqs. (14a) and (14b). The following sections will examine drifts in nonuniform fields by applying this framework and averaging out the gyromotion to understand guiding center drifts.[10]

A. Magnetic field with a spatial gradient, the ∇B Drift.

The ∇B drift occurs as a result of a spatial gradient in the magnetic field strength.[15] When a charged particle moves in a region where the magnetic field is weaker, its gyroradius will increase according to Eq. 6. Likewise, its gyroradius will become smaller when it moves in regions of stronger magnetic field. This asymmetry in the gyroradius means that the particle travels farther and spends more time in regions where the magnetic field is weaker, which leads to a drift of the guiding center in a direction perpendicular to both $\vec{B}$ and ∇B. An example of this is shown in Fig. 4(a). Here, a proton is given an initial velocity in the x-direction in a region where the magnetic field points in the z-direction and linearly increases in the x-direction, *i.e.* $\vec{B} = B(x)\,\hat{z}$. Based on what was observed in Sec. III, the particle will orbit around the magnetic field in the $x-y$ plane and, because of the spatial variation in the magnetic field, the particle will drift in the direction perpendicular to both $\vec{B}$ and ∇B, *i.e.* the $+y$-direction. A side view of the motion is shown in Fig. 4(b).

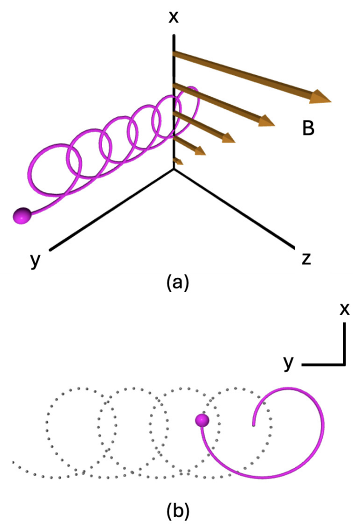

FIG. 4. (a) Plot of the trajectory of a proton in a region where the magnetic field increases linearly, *i.e.* $\vec{B} = B_0 x\,\hat{z}$ T. The particle drifts in the y-direction, *i.e.* the direction of $\vec{B}\times\nabla B$. (b) The particle gyrates about the z-axis, while the guiding center moves in the positive y-direction.

In order to derive an expression for this motion, consider a magnetic field pointing in the $\hat{z}$-direction with straight, parallel field lines, and a strength that varies spatially. To understand how the gradient in the magnetic field influences particle motion, we first examine how the magnetic field changes across a single cyclotron orbit. If we assume that the gradient in the magnetic field is small, we can approximate the field near the guiding center by expanding it in a Taylor series about $\vec{x}_{gc}$. The first two terms in the expansion give: $\vec{B}(\vec{x}) \approx \vec{B}(\vec{x}_{gc}) + (\vec{r}_L\cdot\nabla)\vec{B}$. Using this approximation and Eq. 14b, the Lorentz force equation becomes

$$\vec{F} = m\left[\frac{d\vec{v}_{gc}}{dt} + \frac{d\vec{v}_L}{dt}\right] = q(\vec{v}_{gc}+\vec{v}_L)\times\left[\vec{B}(\vec{x}_{gc}) + (\vec{r}_L\cdot\nabla)\vec{B}\right]. \tag{15}$$

The oscillatory components, $\vec{r}_L$ and $\vec{v}_L$, will have solutions of the form $\vec{r}_L = r_L\left[\sin(\omega_c t)\,\hat{x} + \cos(\omega_c t)\,\hat{y}\right]$, as given in Eq. 7, and $\vec{v}_L = v_L\left[\cos(\omega_c t)\,\hat{x} - \sin(\omega_c t)\,\hat{y}\right]$. Expanding Eq. 15 and averaging each term over a cyclotron orbit, we find that terms linear in gyromotion vanish, as the orbit-averaged values of $\sin(\omega_c t)$ and $\cos(\omega_c t)$ are zero. However, terms containing $\sin^2(\omega_c t)$ and $\cos^2(\omega_c t)$ do not vanish, and their averages yield 1/2. As a result, the $\vec{v}_L\times(\vec{r}_L\cdot\nabla)\vec{B}$ term becomes $-\frac{mv_\perp^2}{2qB}\nabla B$ and the force associated with a gradient in a magnetic field reduces to[10]

$$\vec{F} = -\frac{mv_\perp^2}{2B}\nabla B. \tag{16}$$

Substituting Eq. 16 into Eq. 12 gives a drift velocity of

$$\vec{v}_D = \frac{1}{q}\frac{mv_\perp^2}{2B}\frac{\vec{B}\times\nabla B}{B^2}. \tag{17}$$

This result is consistent with the simulation in Fig. 4. In this example, $\vec{B}$ and ∇B are in the $\hat{z}$ and $\hat{x}\,\hat{y}$ directions, respectively, and the drift motion is in the $\vec{B}\times\nabla B$ direction according to Eq. 17.

B. Magnetic fields with curvature, the Curvature Drift

When a charged particle moves through a region with a curved magnetic field, its guiding center will travel along the curved field lines, causing the particle to experience a centrifugal force that pushes it outward. This force, which is perpendicular to the magnetic field, results in a drift according to Eq. 12.

Figure 5 shows a simulation of two oppositely charged particles moving in a constant magnetic field (represented by concentric rings) that acts circumferentially around the axis of a cylinder. The particles are given initial velocities parallel to the magnetic field. Here, we observe that the particles gyrate around the magnetic field lines, but drift vertically in the $\pm z$-direction for positive/negatively (blue/red) charge particles. As the particles move, the magnetic field curves away from the particles, creating a radial component of the velocity that is perpendicular to the magnetic field. This causes the particles to gyrate around the field line. For the positively charged particle, the gyroradius is larger on the outside of the curve because of the larger velocity component $v_\perp$. The gyroradius is slightly smaller when the particle is closer to the center of the cylinder, and this slight difference in radius causes the positively charged particle to drift upward. A negatively charged particle will gyrate around the field lines in the opposite direction, which causes a drift downwards.

In order to derive the curvature drift velocity, let's assume that the magnetic field points in the $+z$-direction and is curved with a constant radius of curvature, R_c. For simplicity, we neglect any gradients in the magnetic field, since we have already seen their effect on particle motion in Eq. 17, and the net drift can be found by adding the individual drifts that a particle experiences. We also average over a gyroperiod to remain consistent with the earlier derivation. In this case, we only need to consider the motion along the magnetic field. While the particle gyrates around the magnetic field lines, its guiding center will travel in a circle of radius R_c. This results in the particle experiencing a centrifugal force in the radial direction, and the average force is given by Eq. 18.

$$\left\langle \vec{F}_c \right\rangle = \frac{m v_{\parallel}^2}{R_c}\hat{r}, \tag{18}$$

where $v_{\parallel}$ is the velocity parallel to the magnetic field. Since the particle experiences a force, there will be a resulting drift velocity that is perpendicular to the plane formed by the radial direction and the magnetic field. Substituting Eq. 18 into Eq. 12 yields

$$\vec{v}_D = \frac{\vec{F}\times\vec{B}}{qB^2} = \frac{m v_{\parallel}^2}{qB^2}\frac{\vec{R}_c\times\vec{B}}{R_c^2}, \tag{19}$$

where $\vec{R}_c$ is the radius of curvature of the magnetic field and points in the $\hat{r}$ direction.

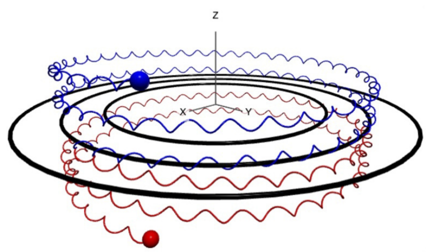

FIG. 5. Charged particles in a curved magnetic field drift in the $\vec{R}_c \times \vec{B}$ direction, with opposite charges drifting in opposite directions. Positive charges (shown in blue) drift up, while negative charges (shown in red) drift down.

C. Magnetic fields with a spatial gradient and curvature, the Toroidal Drift

Gradient and curvature drifts typically occur together and an example of this can be seen in a tokamak, one of the two dominant approaches to magnetic fusion. Here, a toroidal magnetic field is created by a set of current-carrying coils surrounding the tokamak, as shown in Fig. 6, to force the particles to circulate around the torus. The toroidal magnetic field can be calculated using Ampere's law:[16]

$$\vec{B}_T = \frac{\mu_0 N I}{2\pi R}\hat{\phi}, \tag{20}$$

where N is the number of coils used to generate the external (toroidal) magnetic field, I is the current in each coil, R is the distance from the center of the torus to a point inside the torus (a distance known as the *major radius*), and $\hat{\phi}$ is the direction around the torus. The toroidal magnetic field given in Eq. 20 has both a spatial gradient and curvature, so particles in tokamak plasmas will experience the drifts given by Eq. 17 and 19. Since the particle motion will depend on the sign of the particle charge, positive charges will drift in one direction while negative charges will drift in the opposite direction, resulting in charge separation. Thus, in a tokamak, the gradient and curvature drifts combine to cause the particles to drift in the vertical direction and escape . This charge separation also creates an electric field, which when combined with the toroidal magnetic field, can cause the particles to drift radially outward according to the $\vec{E}\times\vec{B}$ drift given in Eq. 11. To account for this, tokamaks include an additional poloidal magnetic field to compensate for this drift and improve confinement.

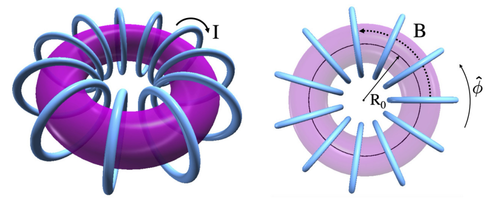

FIG. 6. A set of current-carrying coils, shown in blue, generates a toroidal magnetic field that wraps around the tokamak.

D. Application: Magnetic Mirroring

In Section IV A, we examined how particles drift in regions where the magnetic field gradient has a component perpendicular to the field. Here, we consider a scenario where the gradient is parallel to the field lines and, for simplicity, that the field is rotationally symmetric about a central field line, Fig. 7, which we define to be the $z-$axis. In this situation, the guiding center of the particles will move along the $z-$axis but the particles will experience a constant force that comes from the radial component of the magnetic field, $q\left(v_{\perp}\times B_r\right)$. This force will point in the direction of weaker magnetic field, causing the particle to slow as it moves into the region where the magnetic field is stronger (*i.e.* where the field lines are more concentrated) and eventually reverse their motion, causing the particles to reflect. This is known as magnetic mirroring, and it results in the particle retracing its path along the field lines. This effect is relevant for particle motion in magnetic mirror devices such as the one employed by Realta Fusion.[17] A similar phenomenon occurs in Earth's magnetic field, where the dipole field acts as a natural magnetic mirror, reflecting charged particles between mirror points near the poles.[18]

To illustrate this effect, consider the magnetic field generated between two current-carrying coils placed some distance apart as shown in Fig. 7, which produces curved magnetic field lines that are axisymmetric about the z-axis with both radial, B_r, and axial, B_z, components. The magnetic field strength is highest at the coil centers and reaches a minimum halfway between them, forming a magnetic trap that can confine charged particles. One such field can be described analytically[10] using Eq. 21.

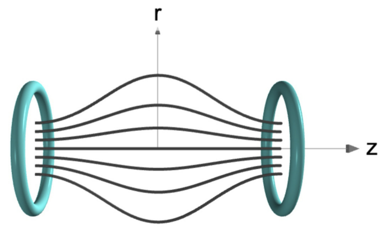

FIG. 7. Illustration of the magnetic field lines between two current-carrying coils. The field lines spread out midway between the coils, indicating a region of minimum magnetic field strength. The field lines converge at the coil centers, where the field strength is at a maximum.

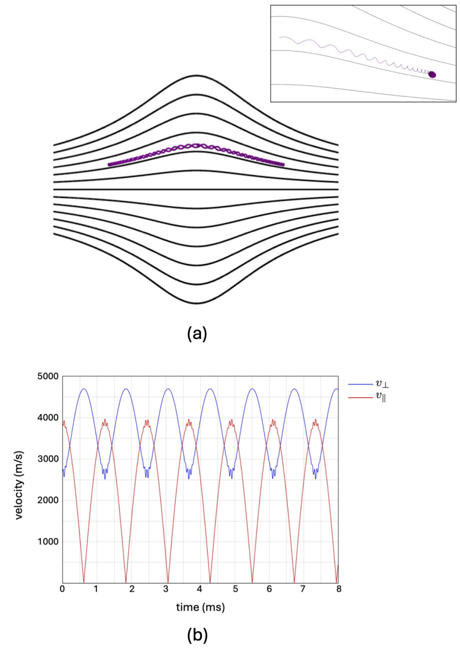

FIG. 8. (a) Simulation of a proton trapped in magnetic mirror with a magnetic field given by Eq. 21. The particle follows the field lines, reflecting once at a point for $z > 0$ and again at $z < 0$. The inset shows a close-up view of the particle as it approaches the mirror point. (b) Plots of $v_\parallel$ and $v_\perp$ showing that $v_\parallel$ goes to zero and $v_\perp$ reaches a maximum at the mirror points.

$$\vec{B} = B_0 \left[-\frac{rz}{L^2}\hat{r} + \left(1 + \frac{z^2}{L^2}\right)\hat{z} \right], \tag{21}$$

where z is the axial distance, r is the radial distance from the axis, L is a characteristic length of the system, and B_0 is the field strength along the centerline at $z = 0$. This field formulation satisfies Maxwell's equation that the field be divergence-free, $\nabla \cdot \vec{B} = 0$, and provides an analytic expression for the magnetic field, eliminating the need to find the magnetic field by numerically integrating the Biot-Savart Law[16] at each location in space.

A simulation of a proton moving in this field is shown in Fig. 8. The proton starts at $z = 0$ and is given an initial velocity with components that are both parallel and perpendicular to the magnetic field. The particle spirals around the field lines, reaches a mirror point in the region $z > 0$, and is reflected back along its original trajectory. After reaching a second mirror point at $z < 0$, it is reflected again, continuing along its path and repeating the cycle. A close-up of the motion near the reflection point shown on the right in Fig. 8 illustrates how the particle trajectory changes as it approaches a region of higher field strength. The helical motion is initially stretched out because the particle has an initial velocity with a component along $\vec{B}$; however, the particle slows as it approaches the mirror point and the helical path becomes compressed. Plots of $v_\parallel$ and $v_\perp$ are also shown in the bottom right of Fig. 8. At the reflection point, $v_\parallel$ decreases to zero, while $v_\perp$ reaches a maximum.

Using the equation for the magnetic field given by Eq. 21 in the Lorentz force equation, we can see that there is a force acting in the $\hat{z}$ direction, given by

$$F_z = -q v_\theta B_r, \tag{22}$$

where v_θ is the velocity component about the z-axis. The radial component of the magnetic field, B_r, is related to B_z through the divergence-free condition of $\vec{B}$, that is: $\nabla \cdot \vec{B} = \frac{1}{r}\frac{\partial}{\partial r}(rB_r) + \frac{\partial}{\partial z}B_z = 0$. If we prescribe the longitudinal gradient $\frac{\partial}{\partial z}B_z$ at $r = 0$ and assume that it is approximately constant, we can integrate the condition that the magnetic field is divergence free to find B_r:

$$B_r = -\frac{r}{2}\frac{dB_z}{dz}. \tag{23}$$

Substituting this into the force equation, Eq. 22, we obtain

$$F_z = q v_\theta \frac{r}{2}\frac{dB_z}{dz}. \tag{24}$$

Near the z-axis, r represents the cyclotron radius given in Eq. 6, such that

$$F_z = -\frac{m v_\perp^2}{2B}\frac{dB_z}{dz} = -\mu \frac{dB_z}{dz}, \tag{25}$$

where μ is the magnetic moment and is given by

$$\mu = \frac{m v_\perp^2}{2B}. \tag{26}$$

Eq. 25 is consistent with Eq. 16, which describes the force arising from a gradient in the magnetic field. This mirror force can thus be written more generally as:

$$F_{\parallel} = -(\mu \nabla B) \cdot \hat{B}, \tag{27}$$

where $\hat{B}$ is the unit vector in the direction of the magnetic field. Returning to Eq. 25 and taking the z-direction to be nearly parallel to $\vec{B}$, we can write the equation of motion as

$$m\frac{dv_{\parallel}}{dt} = -\mu\frac{dB_z}{dz}. \tag{28}$$

Since no electric fields are present and magnetic field do no work, the total kinetic energy is conserved, and we can write

$$\frac{d}{dt}\left(\frac{1}{2}mv_{\parallel}^2 + \frac{1}{2}mv_{\perp}^2\right) = 0. \tag{29}$$

Differentiating this expression and using Eqs. 26 and 28 along with $v_{\parallel} = dz/dt$, we obtain

$$mv_{\parallel}\frac{dv_{\parallel}}{dt} + \frac{d}{dt}(\mu B) = -\mu\frac{dB_z}{dz}\frac{dz}{dt} + \mu\frac{dB}{dt} + B\frac{d\mu}{dt} = 0. \tag{30}$$

The first two terms on the right-hand side of Eq. 30 cancel, leaving

$$\frac{d\mu}{dt} = 0, \tag{31}$$

and therefore, we see that μ is conserved.[9]

Because of the invariance of μ, we can see that $v_{\perp} \propto \sqrt{B}$. This means that as a particle moves into regions of stronger magnetic field, $v_{\perp}$ increases and, to conserve total kinetic energy (assuming $E = 0$), this increase is balanced by a decrease in $v_{\parallel}$. If $v_{\parallel}$ drops to zero, the particle reflects and reverses direction along the field line. This means that the initial conditions play a crucial role in whether the reflection will occur and at what location the reflection will occur. To see this, suppose that a particle starts at an initial position with magnetic field B_i and an initial speed v_0 with a perpendicular velocity component $v_{\perp_0}$. At the reflection point, $v_{\parallel}$ drops to zero, and all of the particle's kinetic energy is contained in $v_{\perp}$, as shown in Fig. 8, meaning that at reflection, $v_{\perp} = v_0$. Using the fact that μ is conserved, we can equate μ at the initial and reflection point to relate the velocity and magnetic field at these location. Doing this tells us that the mirror effect occurs for particles when

$$\left(\frac{v_{\parallel_0}}{v_{\perp_0}}\right)^2 \leq \frac{B_{\max}}{B_i} - 1, \tag{32}$$

where $B_{\max}$ is the magnitude of the magnetic field at the point of reflection, B_i is the initial magnitude of the magnetic field experienced by the particle.

1. *Adiabatic Invariants*

Readers who might be farther along in their physics studies may appreciate an alternative viewpoint for understanding this motion based on adiabatic invariants. In classical mechanics,[19,20] for a system exhibiting periodic motion, the action interval, $\oint p\,dq$, over one oscillation is constant, where p and q are the generalized momentum and generalized coordinate, respectively. This can be even be true in cases when there is a slow change to the system (*i.e.* the rate at which the system changes is slow compared to the period of the motion of interest). In these situations, the associated action integral is no longer a strict invariant but instead an adiabatic invariant and can be a conserved quantity. A plasma in a magnetic mirror exhibits three types of periodic motion and, as a result, has three adiabatic invariants.[9–12] The first adiabatic invariant arises from the gyromotion of the particle around the magnetic field. Here, the generalized momentum is the angular momentum, $mv_{\perp}r$ and the generalized position is the angle that the particle has traversed around the magnetic field, θ. Here, $\oint p\,dq = \oint mv_{\perp}r_L d\theta = 2\pi r_L mv_{\perp} = \frac{2\pi m^2 v_{\perp}^2}{qB} = 4\pi\frac{m}{q}\mu$.Thus, the conservation of μ previously seen is a consequence of the gyromotion of the particle around the magnetic field provided that $\omega \ll \omega_c$. The second periodic motion corresponds to the particle bouncing between the mirror points, which happens at a longer timescale than the gyromotion. Here, the generalized momentum corresponds to the (linear) momentum along the magnetic field, $mv_{\parallel}$, and the generalized coordinate is the distance the gyrocenter travels along the magnetic field, ds. Since the guiding center drifts across magnetic field lines, the motion is not exactly periodic, but it is still a constant of the motion and is known as the longitudinal invariant, $J \equiv \int_a^b v_{\parallel}\,ds$, where a and b correspond to the mirror (turning) points. The third type of periodic motion corresponds to the drift of the gyrocenter across magnetic field lines. Over a much longer period of time, the gyrocenter will exhibit periodic motion across the magnetic mirror and result in a third invariant known as the flux invariant, ϕ. This adiabatic invariant represents the magnetic flux enclosed by the surface enclosed by the bouncing trajectory. Because the timescale of the periodic motion is quite long, it is less likely that the system will change at a rate that is slow compared to the timescale of this motion, and therefore may not satisfy the condition necessary for ϕ to be conserved. As a result, it tends to not be used in calculations.

2. *Wave-Particle Interactions*

In a collisionless plasma, particle-wave interactions can cause an exchange of momentum and energy, resulting in particle diffusion, transport, and scattering. In particular, and relevant to the discussion here, waves can alter the particle pitch angle, $\tan\alpha = v_{\perp}/v_{\parallel}$ through resonant interactions, which may scatter them into the loss cone of a magnetic mirror configuration where they are no longer reflected by the mirror.

Resonance occurs when the wave frequency matches one of the natural frequencies of particle motion (or its harmonics), e.g., the cyclotron frequency. The condition for resonance is[21]

$$\omega - \mathbf{k}\cdot\mathbf{v} = n\omega_c, \tag{33}$$

where ω is the wave frequency, $\mathbf{k}$ is the wave vector, $\mathbf{v}$ is the particle velocity, and n is some integer. When $n=0$, Landau damping occurs, in which a plasma wave is damped by these wave-particle interactions.[22] The adiabatic invariants discussed above hold when changes are slow compared with the period of the cyclotron motion. However, ω is not small compared with ω_c in the case of resonant interactions, and therefore, the adiabatic invariant μ is not conserved.[21]

For more information, we refer the reader to several papers. Tsurutani and Lakhina present an introduction to wave-particle interactions in a collisionless plasma, covering effects such as cyclotron resonance, pitch-angle scattering, and cross-field diffusion.[21] Additional papers discuss in more detail the effects of chorus, a right-hand, circularly-polarized electromagnetic wave, in the magnetosphere on pitch-angle transport.[23,24] Bellan presents a relativistic pseudo-potential model to explain how circularly polarized waves interact with gyrating particles, and applies this work to show that electrons in the magnetosphere can experience large changes in pitch-angle through interactions with whistler waves.[25]

V. TIME-VARYING FIELDS

In the previous sections, we considered what happens to a particle that moves in uniform and spatially varying electric and magnetic fields. However, there are situations in which the fields vary in time. Such situations are relevant in laboratory plasmas when the electromagnetic fields are turned on/off, in radio frequency fields (such as those found in many industrial applications), in laser-driven plasmas, and when electromagnetic waves travel through a plasmas. In this section, we consider two cases with time-varying electric fields.

A. Time-varying Electric and Uniform Magnetic fields, the Polarization Drift

Let's now consider the case where there is a temporally varying electric field, $\vec{E} = E_x(t)\,\hat{x}$, that is perpendicular to a uniform magnetic field, $\vec{B} = B_0\,\hat{z}$. Based on what we saw in Section III B, we would expect to see gyromotion about the guiding center due to the external magnetic field. However, unlike when the electric field is constant, the time varying electric field will result in an acceleration that varies systematically around the cyclotron orbit and will not average to zero like it does when the electric field is constant. This will result in a net shift of the guiding center in the direction of $d\vec{E}/dt$ and the shift will be in opposite directions for positive/negative charges.

For simplicity, let's consider the case where the electric field increases at a constant rate, *e.g.* $E_x(t) = kt\hat{x}$, and assume that the electric field changes at a rate that is slow compared to the timescale of the cyclotron motion. This latter assumption allows us to resolve the motion into two different time-scales: a rapid time-scale corresponding to the cyclotron motion and a slow time-scale that corresponds to the variation in the electric field. Applying the Lorentz force equation yields

$$\dot{v}_x = \frac{q}{m}\left(E(t) + v_y B_0\right) \tag{34a}$$

$$\dot{v}_y = -\frac{qB_0}{m} v_x. \tag{34b}$$

These can be decoupled as we have done before, which leads to

$$\ddot{v}_x = -\omega_c^2\left(v_x \mp \frac{1}{\omega_c}\frac{\dot{E}_x(t)}{B_0}\right) \tag{35a}$$

$$\ddot{v}_y = -\omega_c^2\left(v_y + \frac{E_x(t)}{B_0}\right), \tag{35b}$$

where the upper/lower sign in Eq. 35a corresponds to positive ions/negative electrons. As seen in Eq. 14b, the first term in Eqs. 35a and 35b corresponds to gyromotion around the guiding center, while the second term in Eqs. 35a and 35b corresponds to the motion of the guiding center which has two components. The y-component of the guiding center motion, the second term in Eq. 35b, is perpendicular to $\vec{E}$ and $\vec{B}$ and thus contributes to the usual $\vec{E}\times\vec{B}$ drift. The x-component of the guiding center motion, the second term in Eq. 35a, however, represents a new drift for the guiding center that is in the direction of the electric field and is known as the polarization drift:

$$v_p = \pm\frac{1}{\omega_c}\frac{\dot{E}_x(t)}{B_0}. \tag{36}$$

By inspection, we can make a few observations. First, this drift will result in the ions and electrons moving in opposite directions, which results in a net current given by $\vec{j}_p = n_0 q_e\left(\vec{v}_{p,i} - \vec{v}_{p,e}\right) = \frac{n_0(m_e+m_i)}{B^2}\frac{d\vec{E}}{dt}$ that is in the direction of the electric field and depends on the rate of change in the electric field. Second, because this drift velocity is proportional to the mass, this drift is negligible for electrons. For example, if we consider a hydrogen plasma, the polarization drift velocity of ions is ~ 2000 times larger than for the electrons. Finally, the polarization drift depends on the rate at which the electric field is changing. For example, if the electric field is increasing linearly, the particles will experience an $\vec{E}\times\vec{B}$ drift while the particle's guiding center will follow a parabolic trajectory which then drives a polarization current, as seen in Fig. 9.

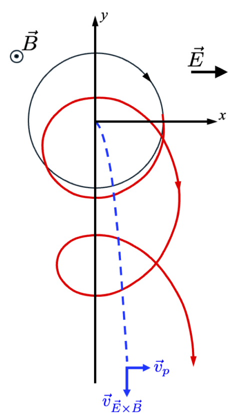

FIG. 9. Sketch depicting the motion of an ion with $E\vec{(t)} = kt\hat{x}$ and $\vec{B} = B_o\hat{z}$. Initially, the electric field is zero and the guiding center is stationary (black curve). When the electric field is turned on at $t = 0$, the particle moves according to the red curve. The guiding center moves in the $-y$ direction due to the $\vec{E}\times\vec{B}$ drift, $\vec{v}_{\vec{E}\times\vec{B}}$, and in the x-direction due to the polarization drift, $\vec{v}_p$, (blue curve).

B. Spatially and Temporally varying Electric Fields, the Pondermotive Force

As a final example, let's consider the motion of a plasma particle in a spatially and temporally varying electric field, $\vec{E} = E(x)\cos(\omega t)\,\hat{x}$. Because the ions have a much larger inertia than the electrons, *i.e.*, $\frac{m_{ion}}{m_e} \gg 1$, they typically are not able to respond on the timescales of the frequencies of the time-varying electric fields that may appear in a plasma and we can focus our attention on the behavior of the electrons. Given that, suppose that an electron is in a spatial region where the electric field is positive and let's consider the motion of the electron during the three parts of the time-varying cycle. During the first part of the cycle ($\omega t < \frac{\pi}{2}$), the electric field initially points in the positive direction and the electron will experience a force that pushes the electrons into a spatial region where the electric field is smaller in magnitude. During the next phase of the cycle ($\frac{\pi}{2} < \omega t < \frac{3\pi}{2}$), the electric field points in the negative direction and the electron will experience a force that causes it to slow before being pushed back into a spatial region where the electric field is larger in magnitude. However, because it is starting in a region where the magnitude of the electric field is smaller, it will experience a smaller force that it did in the first part of the cycle. During the final part of the cycle ($\frac{3\pi}{2} < \omega t < 2\pi$), the electric field is positive again and the electron will again be pushed into a region where the electric field is smaller in magnitude. If we consider this over the whole cycle, the variation in strength of the force on the electron will result in the electron experiencing a net displacement into a region where the electric field is smaller.

To be more quantitative about this, we again start with the Lorentz Force Law, which gives

$$\dot{v}_x = \frac{q}{m}E(x)\cos(\omega t). \tag{37}$$

Eq. 37 can not be solved analytically, but we can gain insight through perturbation theory by performing a Taylor series expansion around the starting position of the electron, x_o, and keeping terms to second order. To do this, we note that $x(t) = x_0 + x_1(t) + x_2(t^2)$ and $E(x) \approx E(x_0) + x_1(t)\frac{dE}{dx}|_{x=x_0}$, where the subscripts 1 and 2 are used to keep track of the order of the terms in the Taylor series expansion. We have assumed that the electric field is to be of first order, which means that the product $x_1(t)\frac{dE}{dx}|_{x=x_0}$ is of second order and no contribution from x_2 is required. After collecting terms, to first order, Eq. 37 becomes

$$\ddot{x}_1 = \frac{q}{m}E(x_o)\cos(\omega t). \tag{38}$$

Eq. 38 can be integrated to obtain the trajectory, $x_1(t) = -\frac{q}{m\omega^2}E_{x_0}\cos(\omega t)$, which exhibits oscillatory motion about the initial location of the electron. A more interesting result can be found when looking at the second order term:

$$\ddot{x}_2 = \frac{q}{m}x_1(t)\left.\frac{dE}{dx}\right|_{x=x_0}\cos(\omega t) \tag{39}$$

$$= -\frac{q^2}{m^2\omega^2}E(x_0)\left.\frac{dE}{dx}\right|_{x=x_0}\cos^2(\omega t). \tag{40}$$

Using the trigonometric identity, $\cos^2 x = \frac{1}{2}(1+\cos 2x)$, and a property of the derivative, $\frac{dg^2(x)}{dx} = 2g(x)\frac{dg(x)}{dx}$, Eq. 40 can be simplified to

$$\ddot{x}_2 = -\frac{q^2}{4m^2\omega^2}\left.\frac{dE^2}{dx}\right|_{x=x_0}(1+\cos 2\omega t). \tag{41}$$

Here we see that the electron experiences a fast acceleration at 2ω, which averages to zero over a cycle, and a mean acceleration that will change the particle's motion. This corresponds to what is known as a ponderomotive force, given by:

$$F_p = -\frac{q^2}{4m^2\omega^2}\left.\frac{dE^2}{dx}\right|_{x=x_0}, \tag{42}$$

where the minus sign tells us that the electron will be driven into regions of smaller electric field.
Application: This simplified model provides an initial understanding of the behavior of electrons in radio frequency fields, such as those found in many industrial applications, and in laser-driven plasmas, where the laser intensity is large enough to ionize the gas. In the latter case, when the frequency of the laser exceeds the plasma frequency, the laser will exert a

pondermotive force on the electrons that pushes them from the center of the beam to a region where the electric field is smaller. This reduces the electron density in the region where the laser beam is present. Since electron density and the refractive index are inversely related, the index of refraction will be larger near the center of the beam. The plasma now acts as a waveguide for the laser, and the beam will self focus as it propagates. This is similar to what occurs in optical fibers, where light travels in a core that is surrounded by a medium with a lower index of refraction.

VI. CONCLUSIONS

The motion of a single charged particle in electromagnetic fields provides a foundational model in the hierarchy of models used to describe and understand plasma behavior. Although this model neglects collective effects arising from collisions, interparticle interactions, and the resulting self-consistent evolution of the electromagnetic fields, this approach still offers rich physical insight into many fundamental processes and applications. In this paper, we derived analytic expressions for several types of drift motion, all of which occur when a charged particle interacts with a combination of externally applied electric and magnetic fields. These include the $\vec{E} \times \vec{B}$ drift, curvature and ∇B drifts, toroidal drift, magnetic mirroring, polarization drift, and the ponderomotive force. In general, we observed that the particle's trajectory can be described as a fast gyromotion about the guiding center, due to the magnetic field, that is superimposed on a net drift motion of the guiding center itself. All of these effects emerge naturally from applying the Lorentz force equation.

Despite the simplicity of the single-particle model, these drifts form the basis for understanding the operation of many plasma devices and applications. Examples include magnetic mirroring, confinement in fusion devices like tokamaks, and particle motion in radiofrequency and laser-driven systems, where the electric field varies with time. A strong understanding of single-particle motion sets the stage for more advanced plasma models, including those that incorporate particle distributions, wave-particle interactions, and self-consistent fields. The reader is encouraged to explore the other papers in this collection to see how single-particle dynamics are integrated into more complex and collective plasma phenomena.

VII. SUPPLEMENTARY MATERIAL

See the supplementary material for the python code used to calculate the values in Table 1 and the majority of the figures in this manuscript.

ACKNOWLEDGMENTS

A.M. Capece acknowledges support by the U.S. Department of Energy Contract No. DE-SC0024656. J. Williams acknowledges support by the U.S. Department of Energy Contract No. DE-SC0021289, the National Science Foundation under Grant No. PHY-2010122 and in part by the National Science Foundation through its employee IR/D program.

[1] A. Dominguez, "Plasma parameters," Physics of Plasmas , under review (2026).
[2] D. Schaffner, "An introduction to plasma science," Physics of Plasmas , under review (2026).
[3] C. Suflee, *The Plasma Universe* (Cambridge University Press, 2013).
[4] M. Cappelli, "The hall effect and rocket flight," Physics Today **62**, 76–77 (2009), https://pubs.aip.org/physicstoday/article-pdf/62/4/76/11091904/76_1_online.pdf.
[5] I. Adamovich, S. Agarwal, E. Ahedo, L. L. Alves, S. Baalrud, N. Babaeva, A. Bogaerts, A. Bourdon, P. J. Bruggeman, C. Canal, and et al., "The 2022 plasma roadmap: Low temperature plasma science and technology," Journal of Physics D: Applied Physics **55**, 373001 (2022).
[6] S. Atzeni, "Fusion energy: from basic research to commercialization," Rendiconti Lincei – Scienze Fisiche e Naturali (2025), 10.1007/s12210-025-01322-8.
[7] B. Srinivasan, "A brief introduction to fusion energy," Physics of Plasmas , under review (2026).
[8] PlasmaPy Community *et al.*, "Plasmapy," (2024).
[9] F. F. Chen, *Introduction to Plasma Physics and Controlled Fusion*, 3rd ed. (Springer International Publishing, 2016).
[10] P. M. Bellan, *Introduction to Plasma Physics and Controlled Fusion* (Cambridge University Press, 2012).
[11] A. Piel, *Plasma physics: An introduction to laboratory, Space, and Fusion Plasmas* (Springer, 2017).
[12] D. A. Gurnett and A. Bhattacharjee, *Introduction to Plasma Physics: With Space, Laboratory and Astrophysical Applications*, 2nd ed. (Cambridge University Press, 2017).
[13] G. Maero, E. D. Hunter, D. J. Murtagh, and E. V. S. and, "Fundamental physics and other applications using nonneutral plasma," Advances in Physics: X **9**, 2367438 (2024), https://doi.org/10.1080/23746149.2024.2367438.
[14] D. H. E. Dubin and T. M. O'Neil, "Trapped nonneutral plasmas, liquids, and crystals (the thermal equilibrium states)," Rev. Mod. Phys. **71**, 87–172 (1999).
[15] A. S. Thrysøe, M. Jessen, E. A. Christensen, M. H. Jørgensen, and S. B. Korsholm, "Measuring grad-b drift in a model of a magnetized torus using a modified helmholtz coil," Physics Education **60**, 045035 (2025).
[16] D. J. Griffiths, *Introduction to Electrodynamics (5th Ed.)*, 5th ed. (Cambridge University Press, 2023).
[17] D. Endrizzi, J. Anderson, M. Brown, J. Egedal, B. Geiger, R. Harvey, M. Ialovega, J. Kirch, E. Peterson, Y. Petrov, and et al., "Physics basis for the wisconsin hts axisymmetric mirror (wham)," Journal of Plasma Physics **89**, 975890501 (2023).
[18] M. K. Öztürk, "Trajectories of charged particles trapped in earth's magnetic field," American Journal of Physics **80**, 420–428 (2012).
[19] L. Landau and E. Lifshitz, *Mechanics*, 3rd ed. (Pergamon Press, 1976).
[20] H. Goldstein, C. P. Poole, and J. L. Safko, *Classical mechanics*, 3rd ed. (Addison-Wesley, 2002).
[21] B. T. Tsurutani and G. S. Lakhina, "Some basic concepts of wave-particle interactions in collisionless plasmas," Reviews of Geophysics **35**, 491–501 (1997).
[22] B. T. Tsurutani and G. S. Lakhina, "Some basic concepts of wave-particle interactions in collisionless plasmas," Reviews of Geophysics **35**, 491–501 (1997).
[23] B. T. Tsurutani, O. P. Verkhoglyadova, G. S. Lakhina, and S. Yagitani, "Properties of dayside outer zone chorus during hildcaa events: Loss of energetic electrons," Journal of Geophysical Research: Space Physics **114** (2009), https://doi.org/10.1029/2008JA013353.
[24] G. S. Lakhina, B. T. Tsurutani, O. P. Verkhoglyadova, and J. S. Pickett, "Pitch angle transport of electrons due to cyclotron interactions with the coherent chorus subelements," Journal of Geophysical Research: Space Physics **115** (2010), https://doi.org/10.1029/2009JA014885.
[25] P. M. Bellan, "Pitch angle scattering of an energetic magnetized particle by a circularly polarized electromagnetic wave," Physics of Plasmas **20**, 042117 (2013).